

Photodegradation of Poly(ethyleneoxide)/Montmorillonite Composite Films

Patrícia C. Lombardo, Alessandra L. Poli, Miguel G. Neumann, Douglas S. Machado, Carla C. Schmitt

Instituto de Química de São Carlos, Universidade de São Paulo, Caixa Postal 780, 13560-970 São Carlos SP, Brazil

Correspondence to: C. C. Schmitt (E-mail: carla@iqsc.usp.br)

ABSTRACT: Poly(ethyleneoxide) (PEO) composites with SWy-1 montmorillonite were prepared by mixing the polymer and the clay in aqueous colloidal solutions. Thin films of the composites were obtained by solvent evaporation and exposed to 254-nm UV-irradiation. The photodegradation was monitored by FTIR and the chain scission reaction was confirmed by measurement of average molecular weights using size exclusion chromatography. The rate of oxidation of pure PEO was much faster than that of the composites (SWy-1/PEO). The SWy-1 clay stabilizes the polymer against UV irradiation. This stabilization is due to two factors: on one side, the absorption of UV radiation by the clay, and on the other the scattering of the incident radiation by the particles; both contributing to minimize the degradation rate of the PEO present in the composites. © 2012 Wiley Periodicals, Inc. *J. Appl. Polym. Sci.* 000: 000–000, 2012

KEYWORDS: degradation; composites; clay; photodegradation; poly(ethyleneoxide)

Received 23 February 2011; accepted 27 April 2012; published online

DOI: 10.1002/app.37987

INTRODUCTION

Polymer–clay composites are a new class of filled polymers in which clay platelets at the nanometer scale are dispersed in a polymer matrix. Especially, interested are nanocomposites containing low amount of nanometric-sized additive in polymer matrix, usually <5 wt %. The main advantages of these nanocomposites are their improved thermal and mechanical properties, reduced flammability, and better barrier properties comparing to unfilled polymer.^{1–3}

The most commonly used clay is the smectite group mineral such as montmorillonite, which belongs to the general family of 2 : 1 layered silicates. The structure of these silicates consists of layers built up by two tetrahedral silica sheets and a central octahedral sheet of magnesium or alumina. Isomorphic substitution within the layers (e.g., Al³⁺ replaced by Mg²⁺ or Fe²⁺) accounts for the residual charge on the surface of the clay. These layers organize themselves in a parallel way to form stacks with regular gaps between them, called interlayer or gallery. In their pristine form, the excess of negative charge is balanced by hydrated cations (Na⁺, Li⁺, and Ca²⁺) in the interlayer region.⁴

Poly(ethylene oxide) (PEO) is a highly hydrophilic, nonionic, flexible, semicrystalline polymer, which is used in many different applications, e.g., as a drug delivery system, mucoadhesive, dispersant, surfactant, hydrogel, electrolyte solvent in lithium

polymer cell, as well as flocculation and rheology control agent.^{5–7} Clay has also been added to PEO to reduce the crystalline phase to improve its ionic conductivity.⁸

The photo-oxidative degradation is critical to polymer materials in their process and usage. It is even the case in polymer-layered silicate composites. Photo-oxidation is a serious factor concern and its effect on pure polymers has been the subject of studies.^{9,10} The mechanism of PEO photodegradation, both in the solid state and in aqueous solutions was described and discussed in detail by Morlat and Gardette.^{11,12} During the last years, the main attempt concerning nanocomposites has been their preparation and study of its mechanical properties.^{13,14} Despite numerous reports on polymer-layered silicates, very little attention has been paid to the photostability of these nanomaterials.^{15–19}

In the present work, the effect of UV irradiation on PEO/SWy-1 nanocomposites has been investigated.

EXPERIMENTAL

Materials

The montmorillonite clay SWy-1/ Na⁺ (Source Clays Repository of the Clay Minerals Society, University of Missouri, Columbia, MO) was used in this work. The clay was purified as described earlier.²⁰ PEO was supplied by Sigma Aldrich (average molar mass ~100,000).

© 2012 Wiley Periodicals, Inc.

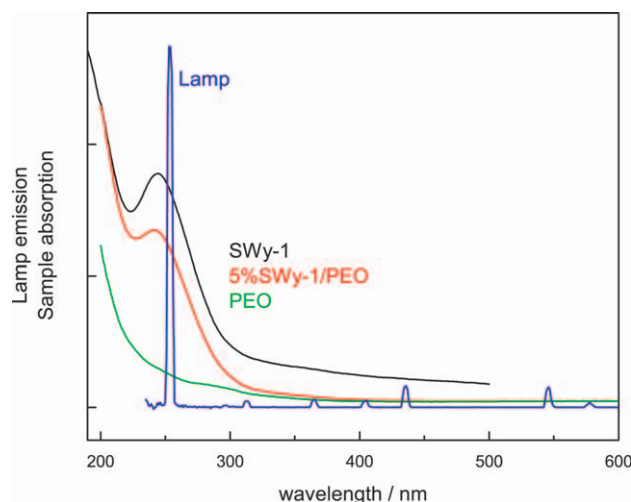


Figure 1. Emission spectra of the irradiating lamp and absorption spectra of PEO, SWy-1, and the composite film. [Color figure can be viewed in the online issue, which is available at wileyonlinelibrary.com.]

Composite Preparation

Clay suspensions were prepared by dispersing the clay in Millipore water (Milli Q) and stirred for 24 h. Afterward, an aqueous solution of PEO (1%, w/v) was added to the clay suspensions. The clay-PEO solutions containing different amounts of SWy-1 (0.5, 1.0, 2.5, and 5.0%) were poured onto glass plates and dried at 37°C. The mixture was then heat-pressed between two aluminium supports for 1 min at 100°C and 14.5 kgf cm⁻². The films were peeled off the aluminum support and stored.

UV-Irradiation

The films were exposed to UV light in an irradiation chamber containing 16 UV germicidal lamps (total power 96 W) at 40°C. The lamps emitted predominantly 254-nm wavelength and the photon flux was 1.78×10^{21} photons/m² s⁻¹. The photon flux was determined using the equation described by Neumann et al.²¹ The emission spectrum of the lamps is shown in Figure 1, together with the absorption spectra of the clay, the polymer, and the composite film. The emission of the lamp was determined using a SPR-01 spectroradiometer (Luzchem). The absorption spectra of the films were recorded on a Shimadzu UV-2550 spectrophotometer, using the film holder of the diffuse reflectance accessory.

Analysis

The intercalated compounds were characterized by X-ray diffraction (XRD) on an Enraf-Nonius Kappa CCD diffractometer (Cu, radiation $\lambda = 0.154$ nm) at 50 kV, 100 mA. The evaluation of the superficial morphology of the compounds was performed by scanning electron microscopy (SEM) using a 20 keV energy ZEISS LEO 440 equipment with an OXFORD 20 kV detector at 2.7×10^{-6} torr. A magnification of 3000 \times was applied. A drop of the dilute dispersion was deposited on an aluminum stub, slowly evaporated, and coated with a gold film of ~ 2 nm.

Photodegradation was followed by Fourier transform infrared spectroscopy (FTIR) (Bomem-100 MB Series spectrometer) with

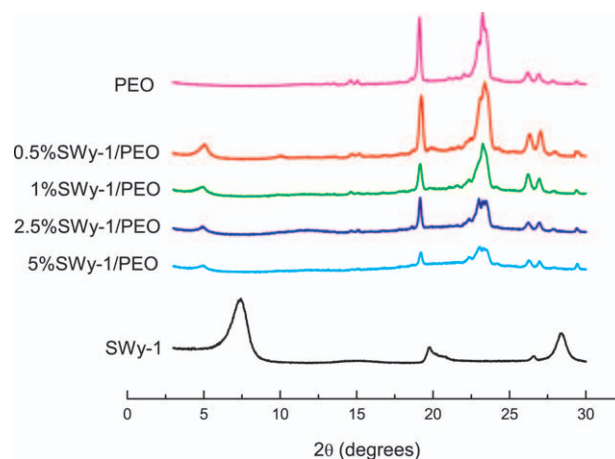


Figure 2. X-ray diffraction for SWy-1 clay, PEO, and composites. [Color figure can be viewed in the online issue, which is available at wileyonlinelibrary.com.]

a Golden Gate single reflection diamond attenuated total reflection (ATR) unit (Specac). The photodegradation of each sample was run in triplicate using pieces cut from different regions of the film.

Average molar masses were determined by size exclusion chromatography (SEC) at 35°C on a Shimadzu LC-10 AD chromatographic system with a Shimadzu RID—6A refractive index detector. Irradiated film samples were dissolved in Milli Q water and 2-mL aliquots filtered through 0.45- μ m filters (Regenerated Cellulose, Sartorius) to remove undesired contaminants. Reminiscent clay particles eventually present in the filtrate did not interfere in the analysis due to their small size and very low concentration. About 20 μ L of the sample solutions were injected in set of three OHPAK KB-806M columns. Millipore (Milli Q) water was used as the eluent at a flow rate of 1 mL min⁻¹. Narrow-distribution PEO standards (American Polymer Standards Corp.) were used for calibration.

RESULTS AND DISCUSSION

Characterization of SWy-1/PEO Composites

The structure of the composites with different amounts of SWy-1 was studied by X-ray diffraction. Figure 2 shows the diffraction patterns of PEO, SWy-1, and PEO composite with different SWy-1 concentrations. The signal for pure SWy-1 shows a peak at $2\theta = 7.4^\circ$, which corresponds to an interlamellar spacing of about 12 Å assigned to the hydrated sample containing a monolayer of H₂O. Table I presents the 2θ values and the interlayer

Table I. Interlamellar Spacings and 2θ Values for Composite Films

	2θ	d (Å)
SWy-1	7.4	11.9
0.5%SWy-1/PEO	5.0	17.7
1.0%SWy-1/PEO	4.9	18.0
2.5%SWy-1/PEO	4.9	18.0
5.0%SWy-1/PEO	5.0	17.7

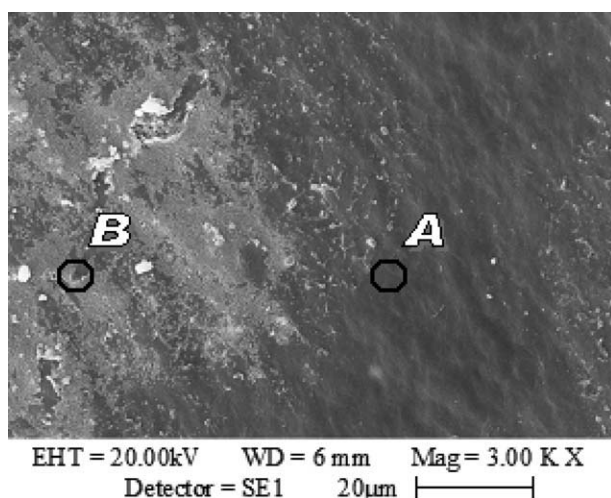


Figure 3. SEM for 5%SWy-1/PEO. EDX analysis was performed at points A and B.

spacing for the SWy-1/PEO composites with different clay contents.

For the SWy-1/PEO composites the signal is shifted to lower 2θ values (5°) corresponding to an interlamellar spacing of about 17.7 Å, compared with 12 Å found for the pure SWy-1. This expansion was assigned to a possible planar zigzag conformation of the PEO chains,²² or to the preservation of the PEO helical conformation in the interlayer region. This interlayer expansion is in good agreement with the results obtained by Aranda et al. in studies of intercalation of PEO in silicates.^{22,23} Wu and Lerner also found that the gallery size increased by around 4 or 8 Å when mono- and bilayers of PEO were intercalated in montmorillonite galleries.²³ On the other hand, it can be seen that the intensity of the crystalline PEO peaks (at 29 and 33°) decrease with increasing amount of clay in the nanocomposites. This may be due to the fact that the polymer loses partially its crystalline structure when intercalated in the clay.²⁴

An overall analysis of the SEM picture shows two regions represented by the dark and light regions, as can be seen in Figure 3. There seems to be an inhomogeneous distribution of clay in the film, showing a reasonable amount of clay islands in the lighter regions. EDX analysis in the B (light) and A (dark) regions showed that the silicon content is about three times larger in the light region (19.0%) than in the dark one (7.0%). Conversely, the carbon content falls by about 50% (B: 56.6% vs. A: 25.6%). As the polymer is formed only by carbon and oxygen atoms and the clay contains heavier elements, like silicon, it is possible to assume a higher polymer content in the dark regions and higher clay content in the light region. Nevertheless, when increasing the clay proportion from 0.5 to 45%, practically no change in the degradation rate was observed, indicating that regions with less Si-content contain enough clay to inhibit the photodegradation process.

FTIR spectra of PEO, SWy-1, and 0.5%SWy-1/PEO are shown in Figure 4. Pure PEO exhibits a broad band at 2881 cm^{-1} due to the symmetric stretching of the —CH bond (from the aliphatic CH_2 group in ethyleneoxide).^{25,26} The other characteristic bands observed at 1466, 1342, and 1281 cm^{-1} are assigned to

CH deformation vibrations.²⁷ The peak at 957 cm^{-1} is related to the helical structure of PEO and the peaks in the 1061–1150 cm^{-1} region correspond to the asymmetric stretching of the C—O—C groups.²⁵ Similar bands were found by Kaczmarek et al. for blends of poly(ethyleneoxide) (PEO) and pectin.²⁷ SWy-1 presents broad hydroxyl (O—H) and silanol (Si—O—Si) bands at 3000–3600 and 1000–1200 cm^{-1} , respectively.^{17,28} The spectrum of the 0.5%SWy-1/PEO composite is the combination of the bands of the spectra of both components. It has to be taken into account that the clay content in the composite is roughly 1% of that used in the spectrum of the pure clay which was taken using a pressed sample of pure clay.

Photo-oxidative Degradation of PEO/SWy-1 Composites

The SWy-1/PEO (0.5, 1.0, 2.5, and 5.0%) composites were irradiated with UV light for up to 307 h at 40°C. UV irradiation of SWy-1/PEO films causes significant changes in FTIR spectra, which are shown in Figure 5.

New bands are formed at 1720 and 3430 cm^{-1} . The increase of the band at 1720 cm^{-1} can be attributed to the formation of carbonyl species.^{16,17,27,29} The band at 3430 cm^{-1} also increases during UV irradiation of the composite films. This band is typical of hydroxyl and hydroperoxide groups (OH/OOH).^{28,30,31} The general mechanism for leading to the formation of those groups during the photodegradation of PEO is shown schematically in Scheme 1.²⁷ The shift and change of the shape of the band around 1000 cm^{-1} can be ascribed to the conversion of the crystalline helicoidal form of recently casted PEO to a more amorphous conformation after degradation.³²

Size Exclusion Chromatography (SEC)

For the pure polymer (PEO), as well as for the composites (SWy-1/PEO with 0.5, 1.0, 2.5, and 5.0% clay content), the changes caused by irradiation of the samples are characterized by a decrease of molecular weights. The molecular weights (M_w) of PEO and SWy-1/PEO films are in the range of 60,000

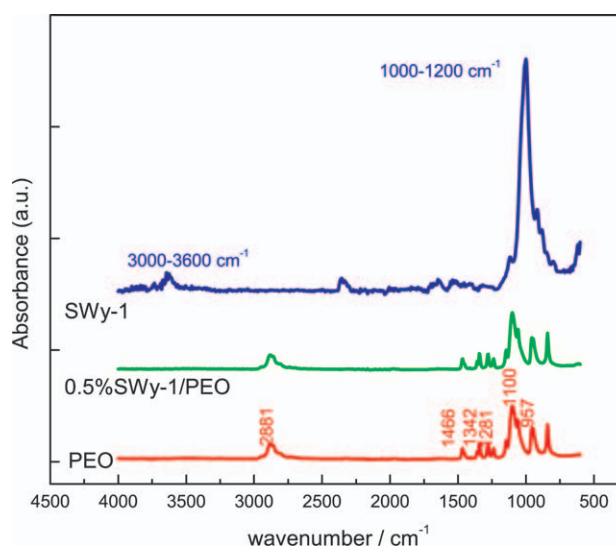


Figure 4. FTIR spectra of PEO, 0.5%SWy-1/PEO composite film, and solid SWy-1. [Color figure can be viewed in the online issue, which is available at wileyonlinelibrary.com.]

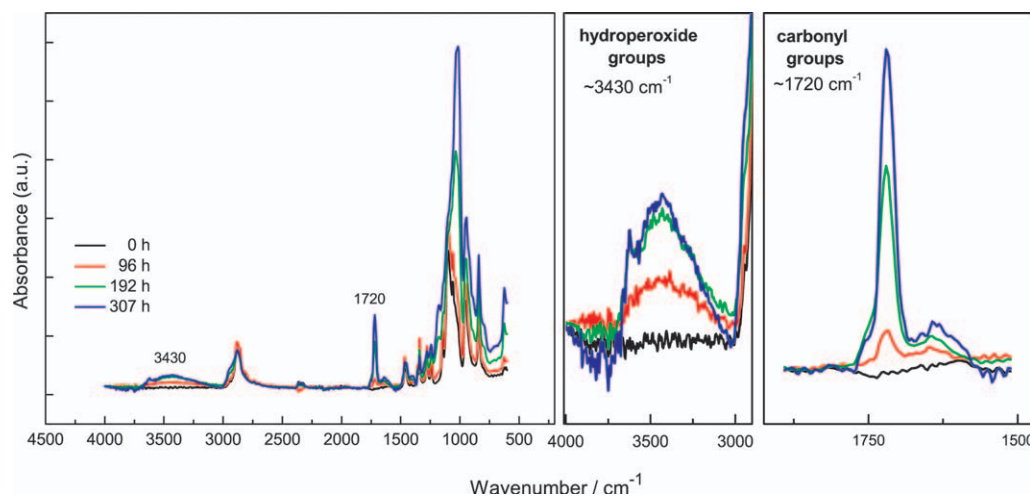


Figure 5. FTIR spectra of 5%SWy-1/PEO composite film as a function of irradiation time. [Color figure can be viewed in the online issue, which is available at wileyonlinelibrary.com.]

and 500,00, respectively. Whereas the M_w of pure PEO was reduced to 50% of its initial value after 3 h of irradiation, the same reduction was only achieved after about 72 h for the SWy-1/PEO (Figure 6).

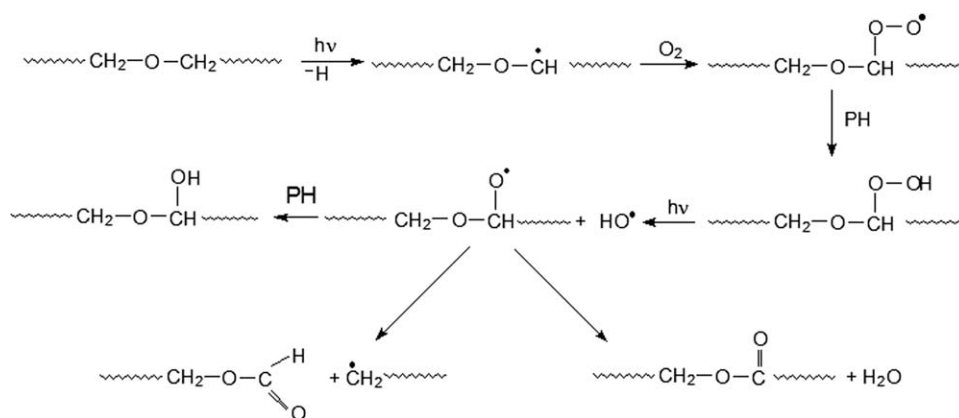
There seems to be no direct relationship between the rate of photodegradation and the clay content, possibly because only a small amount of clay seems to be sufficient to reduce the oxidation process. The differences observed in Figure 6 are possibly due to the experimental error in the determination of M_w . It can be seen that the trend is erratic at different times (by instance, after 25 min the order is exactly the opposite), although the decay without SWy-1 is definitively faster. The polydispersity ($\overline{M}_w/\overline{M}_n$) of the samples before and after irradiation is shown in Table II. Within the experimental error of the procedure (about 10%) it can be considered that the polydispersity is similar for the pure polymer and the composites. There is a decrease of the polydispersity during irradiation, as well as a narrowing of the chromatographic SEC curves indicating that the polymer becomes more uniform in terms of mass distribution. This effect might be due to scissions in preferential sites and rapid formation of low molecular weight products (peaks

at longer retention time appears on the chromatographic curves as a result of irradiation). Similar results were obtained by Morlat et al. for the photo-oxidation of PEO in aqueous solution, where oxidized polymers presented lower polydispersity than the original samples.¹² Although, at the moment, there seems to be no detailed explanation for this finding.

The progress of the PEO degradation processes could also be assessed by the number of average chain scissions per molecule (S). This parameter can be calculated according to the model developed by Madras and McCoy,³³ using:

$$S = \frac{\overline{M}_n(0)}{\overline{M}_n(t)} - 1$$

It can be seen from Table II that the number of scissions per molecule for PEO is higher than for the composites. No clear correlation was found between the amount of clay in the composites and the number of scissions, confirming the finding that a low amount of dispersed clay is sufficient to reduce the oxidation process. A similar conclusion can be reached from the relation between the polydispersity and the clay content.



Scheme 1. Photo-oxidative degradation of PEO.

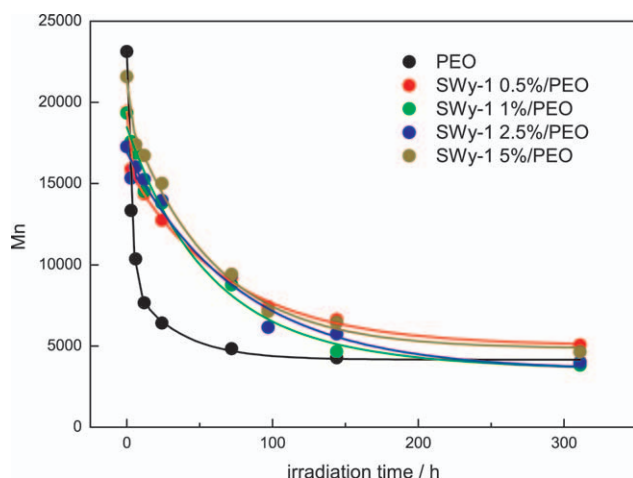


Figure 6. Decrease of the molecular weight (\overline{M}_n) during photodegradation of PEO and composites. [Color figure can be viewed in the online issue, which is available at wileyonlinelibrary.com.]

The model for polymer degradation described by Marimuthu and Madras³⁴ leads to a correlation between the change of the number-average molecular weight M_n with time and the degradation rate constant k_d .

$$\frac{\overline{M}_n(0)}{\overline{M}_n(t)} - 1 = \overline{M}_n(0)k_d t \quad (1)$$

This relationship is plotted in Figure 7. It can be seen that the ratio $\overline{M}_n(0)/\overline{M}_n(t)$ shows an asymptotic behavior, reaching its maximum faster for the pure polymer than for the clay-containing films. The degradation rate coefficients, k_d , for PEO and the SWy-1/PEO films were calculated from the initial slopes of these curves [shown in Figure 7(b)], using the initial M_n for each system. The values are shown in Table III, from where it can be

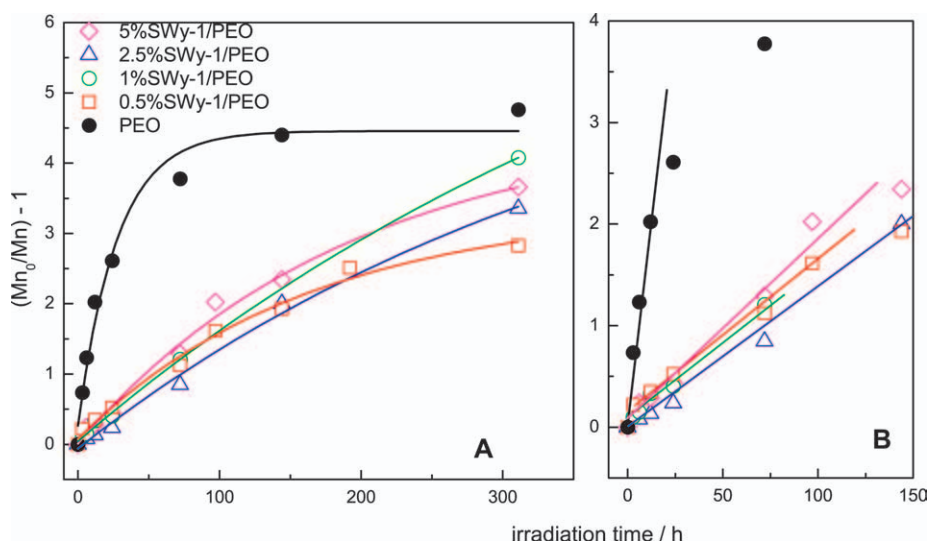


Figure 7. (a) Variation of $[\overline{M}_n(0)/\overline{M}_n(t)] - 1$ vs. irradiation time for the degradation of PEO and SWy-1/PEO composites; (b) blow-up of the initial times. [Color figure can be viewed in the online issue, which is available at wileyonlinelibrary.com.]

Table II. Polydispersitivity and Number of Average Chain Scissions Per Molecule After Irradiation

	t (h)	M_w/M_n	S
PEO	0	2.7	0
	311	1.4	4.8
0.5%SWy-1/PEO	0	2.4	0
	311	1.6	2.8
1%SWy-1/PEO	0	2.5	0
	311	1.2	4.1
2.5%SWy-1/PEO	0	2.7	0
	311	1.1	3.4
5%SWy-1/PEO	0	2.8	0
	311	1.2	3.7

seen that the degradation rate coefficient for pure PEO is about 10 times larger than that for the composites.

The SWy-1 clay can be considered as stabilizer against 254 nm UV irradiation. The stabilization mode of the clay may be explained on the ability of SWy-1 not only to scatter the incident light but also to absorb part of the UV light thus minimizing the absorption by PEO and the degradation of the polymer in the composites. Montmorillonites characteristically show a charge transfer transition in the 241–243 nm range,³⁵ in both films and suspensions, as can be observed in Figure 1. Essawy et al. observed similar effect for the photodegradation of Laponite/PVC composites, where Laponite (a synthetic hectorite-type clay) improved the resistance of the polymer to UV photodegradation.³⁶

These composites might be useful in systems in which the polymers are in rich UV radiation environments, like devices use in spatial research or where UV radiation is used for other applications. On the other hand, it can lead to development of systems

Table III. Initial Number Average Molecular Weights and Photodegradation Rates of PEO and SWy-1/PEO Films

	M_n	k_d (10^{-7} mol g $^{-1}$ h $^{-1}$)
PEO	23,200	70.0
0.5%SWy-1/PEO	19,400	7.3
1.0%SWy-1/PEO	19,400	8.3
2.5%SWy-1/PEO	17,300	8.7
5.0%SWy-1/PEO	21,600	7.8
45%SWy-1/PEO	19,100	5.9

with functionalized clays that could absorb at larger wavelengths.

CONCLUSIONS

PEO can be intercalated into SWy-1 via mixing in aqueous colloidal solutions to produce intercalated SWy-1/PEO composites. Clay aggregates in the film were observed by SEM. The presence of SWy-1 in PEO slowed down the rate of photo-oxidation of the polymer and decreased the main chain scission process. The photodegradation rate of pure PEO is about 10 faster in the absence of clay than for the composites (SWy-1/PEO). The SWy-1 clay can be considered as a stabilizer against 254-nm UV photodegradation. The stabilization mode of the clay may be explained by the ability of SWy-1 not only scatter the incident light but also to absorb the UV light instead of the PEO, thus minimizing the degradation rate of composites.

ACKNOWLEDGMENTS

The authors thank FAPESP (Proc. 2009/15998-1) and CNPq (304672/2011-4 and 303564/2010-5) for financial support. This is a contribution from the USP Research Consortium for Photochemical Technology.

REFERENCES

- Alexandre, M.; Dubois, P. *Mater. Sci. Eng. B* **2000**, *28*, 1.
- Qin, H.; Zhang, S.; Liu, H.; Xie, S.; Yang, M.; Shen, D. *Polymer* **2005**, *46*, 3149.
- Ray, S. S.; Yamada, K.; Okamoto, M.; Fujimoto, Y.; Ogami, A.; Ueda, K. *Polymer* **2003**, *44*, 6633.
- Manias, E.; Touny, A.; Wu, L.; Strawhecker, K.; Lu, B.; Chung, T. C. *Chem. Mater.* **2001**, *13*, 3516.
- Aoki, T.; Konno, A.; Fujinami, T. *Electrochim. Acta* **2004**, *50*, 301.
- Gaudreault, R.; Van de Ven, T. G. M.; Whitehead, M. A. *Colloids Surf. A* **2005**, *268*, 131.
- Serra, L.; Domenech, J.; Peppas, N. A. *Eur. J. Pharm. Biopharm.* **2006**, *63*, 11.
- Burgaz, E. *Polymer* **2011**, *52*, 5118.
- Santos, L. C.; Poli, A. L.; Cavalheiro, C. C. S.; Neumann, M. G. *J. Braz. Chem. Soc.* **2009**, *20*, 1467.
- Guadagno, L.; Naddeo, C.; Vittoria, V. *Macromolecules* **2004**, *37*, 9826.
- Morlat, S.; Gardette, J. *Polymer* **2001**, *42*, 6071.
- Morlat, S.; Gardette, J. *Polymer* **2003**, *44*, 7891.
- Ray, S. A.; Okamoto, M. *Prog. Polym. Sci.* **2003**, *28*, 1539.
- Okada, A.; Usuki, A. *Macromol. Mater. Eng.* **2006**, *291*, 1449.
- Tidjani, A.; Wilkie, C. A. *Polym. Degrad. Stab.* **2001**, *74*, 33.
- Qin, H.; Zhang, Z.; Feng, M.; Gong, F.; Zhang, S.; Yang, M. *J. Polym. Sci. B Polym. Phys.* **2004**, *42*, 3006.
- Kaczmarek, H.; Podgórski, A. *J. Photochem. Photobiol. A* **2007**, *191*, 209.
- Kandilioti, G.; Elenis, A.; MacChiarola, K. A.; Gregoriou, V. G. *Appl. Spectrosc.* **2006**, *60*, 1285.
- Morlat, S.; Mailhot, B.; Gonzalez, D.; Gardette, J. L. *Chem. Mater.* **2004**, *16*, 377.
- Gessner, F.; Schmitt, C. C.; Neumann, M. G. *Langmuir* **1994**, *10*, 3749.
- Neumann, M. G.; Miranda, W. G.; Schmitt, C. C.; Rueggeberg, F. A.; Correa, I. C. J. *Dent.* **2005**, *33*, 525.
- Aranda, P.; Ruiz-Hitzky, E. *Chem. Mater.* **1992**, *4*, 1395.
- Wu, J.; Lerner, M. M. *Chem. Mater.* **1993**, *5*, 835.
- Shen, Z. Q.; Simon, G. P.; Cheng, Y. B. *Eur. Polym. J.* **2003**, *39*, 1917.
- Ratna, D.; Abraham, T. N.; Karger-Kocsis, J. *J. Appl. Polym. Sci.* **2008**, *108*, 2156.
- Volel, M.; Armand, M.; Gorecki, W.; Saboungi, M. L. *Chem. Mater.* **2005**, *17*, 2028.
- Kaczmarek, H.; Bajer, K.; Galka, P.; Kotnowska, B. *Polym. Degrad. Stab.* **2007**, *92*, 2058.
- Morlat-Therias, S.; Fanton, E.; Gardette, J. L.; Dintcheva, N. T.; La Mantia, F. P.; Malatesta, V. *Polym. Degrad. Stab.* **2008**, *93*, 1776.
- Aranda, P.; Mosqueda, Y.; Pérez-Capde, E.; Ruiz-Hitzky, E. *J. Polym. Sci. B Polym. Phys.* **2003**, *41*, 3249.
- Morlat-Therias, S.; Mailhot, B.; Gonzalez, D.; Gardette, J. L. *Chem. Mater.* **2005**, *17*, 1072.
- Neumann, M. G.; Schmitt, C. C.; Goi, B. E. *J. Appl. Polym. Sci.* **2010**, *115*, 1283.
- Marcos, J. I.; Orlandi, E.; Zerbi, G. *Polymer* **1990**, *31*, 1899.
- Madras, G.; McCoy, B. *Chem. Eng. Sci.* **1997**, *52*, 2707.
- Marimuthu, A.; Madras, G. *Ind. Eng. Chem. Res.* **2007**, *46*, 15.
- Karickhoff, S. W.; Bailey, G. W. *Clays Clay Miner.* **1973**, *21*, 59.
- Essawy, H. A.; El-Wahab, N. A. A.; El-Ghaffar, M. A. A. *Polym. Degrad. Stab.* **2008**, *93*, 1472.